A Numerical Analysis of Line Equations Considering Corona Loss on a Single-Conductor System and Its Application

By

Shigenori HAYASHI*, Jūrō UMOTO* and Eishi NAKAMURA**

(Received December 6, 1965)

In this paper, the authors introduce a new digital analysis of the attenuation and distortion of the travelling waves caused by corona discharge on a single-conductor system, which is founded on their surge analyser considering corona loss. Then, applying their theory to the subject of the transient voltage rise of the transmission towers due to lightning stroke on the overhead ground wire, they numerically analyse the subject by a digital computer and discuss the influences of the corona loss on the wire to the tower voltages.

1. Introduction

In order to discuss the surge performances on the transmission systems, for instance, the probability of the inverse flashover along the insulators at the transmission towers due to lightning stroke against the ground wire or tower, it is very important that we investigate not only the wave distortion and attenuation due to the skin effects of the lines and the ground return, but also those caused by the corona discharge from the conductor surface, through the line equations.

In this view, already the authors have invented a surge analyser considering the corona loss, and availing it, they investigated the wave attenuation and distortion due to corona on the transmission lines[1)~4)]. On the other hand, in the recent years, the digital computer technique has been made great strides and also, it is applied, little by little, to the analysis of the surge phenomena on the transmission systems[5) 6)].

Now, in this paper, first the authors present a new numerical analysis of the attenuation and distortion of the travelling waves due to corona loss by means of their surge analyser, in other words, the approximate equivalent circuit of a single-conductor system with the corona loss elements. Then,

* Department of Electrical Engineering, II
** Sumitomo Electric Industries, Ltd.

applying their theory to the problem of the transient voltage rise of the transmission towers due to the lightning stroke on the overherd ground wire, they numerically analyse this subject and discuss how much are the influences of the corona loss on the wire to the tower voltage rise.

2. Numerical Analysis of Line Equations Considering Corona Loss

2.1 Line equations for the case under corona voltage

As is well known, the relations between the voltage v and current i on a single-conductor systems for the case under the corona voltage at the point x and at the instant t as shown in Fig. 1, are given by the following simultaneous line equations:

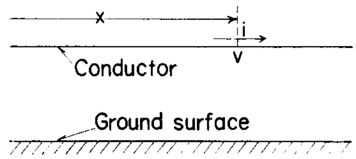

Fig. 1. Illustration of a single-conductor system.

$$\left.\begin{aligned} -\frac{\partial v}{\partial x} &= L\frac{\partial i}{\partial t}, \\ -\frac{\partial i}{\partial x} &= C\frac{\partial v}{\partial t}, \end{aligned}\right\} \qquad (1)$$

where

L, C: inductance and capacitance of line per unit length.

Though in these equations are neglected the skin effects of the conductor and ground return, we shall discuss our subject by means of the proposed equations[1)~4)]. Now, Fig. 2 illustrates an equivalent lumped circuit of a single-conductor system per the ν-th distance increment Δx, i.e. the ν-th element, where $\nu = 1, 2, \cdots, n$. In Fig. 2,

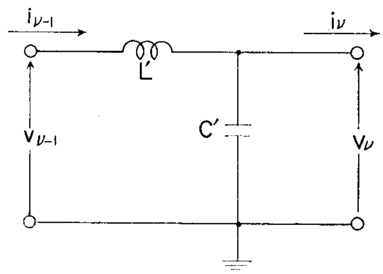

Fig. 2. The ν-th element of an approximate equivalent circuit of a single-conductor system for lower voltage than corona voltage.

$$L' = L\Delta x, \qquad C' = \Delta x,$$

v_ν, i_ν : output voltage and current of the ν-th element, where $\nu = 1, 2, \cdots, n$,

$v_{\nu-1}$, $i_{\nu-1}$: input voltage and current of the ν-th element or output ones of the $(\nu-1)$-th,

n: number of total elements.

Next, according to Eqs. (1), we have the following difference-differential equations conserning x and t for the input and output voltages and currents of the ν-th element in Fig. 2.

$$\left.\begin{aligned} &L'\frac{di_{\nu-1}}{dt} = v_{\nu-1}-v_{\nu}\,, \\ &C'\frac{dv_{\nu}}{dt} = i_{\nu-1}-i_{\nu}\,, \\ &\nu = 1,2,\cdots,n\,. \end{aligned}\right\} \tag{2}$$

From Eqs. (2), we can introduce the next approximate difference equations conserning x and t.

$$\left.\begin{aligned} &L'(i_{\nu-1}-i^0_{\nu-1}) = (v_{\nu-1}-v_{\nu})\,\Delta t\,, \\ &C'(v_{\nu}-v^0_{\nu}) = (i_{\nu-1}-i_{\nu})\,\Delta t\,, \end{aligned}\right.$$

where

$$\left.\begin{aligned} &v^0_{\nu} = v_{\nu}|_{t=t-\Delta t}\,, \qquad t\geq 0\,, \\ &i^0_{\nu-1} = i_{\nu-1}|_{t=t-\Delta t}\,,\ t\geq 0\,, \\ &\nu = 1,2,\cdots,n\,. \end{aligned}\right\} \tag{3}$$

On the other hand, at the final end ($\nu=n$), the relation between the voltage v_n and current i_n will be given by

$$i_n = a^0_{2n}v_n + b^0_{2n}\,, \tag{4}$$

generally, where

a^0_{2n}, b^0_{2n}: constants determined by terminal condition.

Substituting i_n in this equation into the second equation (let $\nu=n$) of Eqs. (3), we can descrive v_n with i_{n-1}. Next substitution v_n into the first equation (let $\nu=n$) gives the expression of i_{n-1} by v_{n-1}. If such treatments are successively repeated, in the results, a set of equations are obtained as follows:

$$\left.\begin{aligned} &v_n = \frac{\Delta t}{C'+a^0_{2n}\,\Delta t}\,i_{n-1} + \frac{C'v^0_n - b^0_{2n}\,\Delta t}{C'+a^0_{2n}\,\Delta t} \\ &\qquad (\equiv a^0_{2n-1}i_{n-1} + b^0_{2n-1})\,, \\ &i_{n-1} = \frac{\Delta t}{L'+a^0_{2n-1}\,\Delta t}\,v_{n-1} + \frac{L'i^0_{n-1} - b^0_{2n-1}\,\Delta t}{L'+a^0_{2n-1}\,\Delta t} \\ &\qquad (\equiv a^0_{2n-2}v_{n-1} + b^0_{2n-2})\,, \\ &\cdots\cdots\cdots\cdots\cdots\cdots\cdots\cdots\cdots\cdots \\ &i_{\nu} = i_{n-\mu} = \frac{\Delta t}{L'+a^0_{2\nu+1}\,\Delta t}\,v_{\nu} + \frac{L'i^0_{\nu} - b^0_{2\nu+1}\,\Delta t}{L'+a^0_{2\nu+1}\,\Delta t} \\ &\qquad (\equiv a^0_{2\nu}v_{\nu} + b^0_{2\nu})\,, \\ &v_{\nu} = v_{n-\mu} = \frac{\Delta t}{C'+a^0_{2\nu}\,\Delta t}\,i_{\nu-1} + \frac{C'v^0_{\nu} - b^0_{2\nu}\,\Delta t}{C'+a^0_{2\nu}\,\Delta t} \\ &\qquad (\equiv a^0_{2\nu-1}i_{\nu-1} + b^0_{2\nu-1})\,, \\ &\cdots\cdots\cdots\cdots\cdots\cdots\cdots\cdots\cdots\cdots \end{aligned}\right\} \tag{5}$$

$$v_1 = v_{n-(n-1)} = \frac{\Delta t}{C'+a_2^0\Delta t} i_0 + \frac{C'v_0^0 - b_2^0\Delta t}{C'+a_2^0\Delta t}$$
$$(\equiv a_1^0 i_0 + b_1^0),$$
$$i_0 = i_{n-n} = \frac{\Delta t}{L'+a_1^0\Delta t} v_0 + \frac{L'i_0^0 - b_1^0\Delta t}{L'+a_1^0\Delta t}$$
$$(\equiv a_0^0 v_0 + b_0^0),$$

where

$\nu = n-\mu, \quad \mu = 0, 1, 2, \cdots, n,$

$\nu = 0$: corresponds to applied end.

Hence, if in Eqs. (5) are given the initial current $i_\nu^{+0} = i_\nu^0$ of the second kind at $t=0$ and v_0 as the applied voltage or a functional relation between i_0 and v_0, all v_ν and i_ν at $t=\Delta t$ are numerically calculated by using Eqs. (5). Moreover, assuming that these v_ν and i_ν at $t=\Delta t$ are the initial voltage and current, v_ν and i_ν at $t=2\Delta t$ are numerically computed by Eqs. (5). The repeats of such digital computations present the values of v_ν and i_ν at any instant in the results.

2.2 Line equations considering corona loss

On the assumption that the formula of the square characteristics for the ac corona loss of the wire given by Peek is yet the appropriate one to the corona loss with respect to travelling waves, the line equations were modified[3)~4)] by the authors, so that the wave attenuation and distortion by the corona loss may be analysed more favourablly than hitherto, as follows:

$$-\frac{\partial v}{\partial x} = L\frac{\partial i}{\partial t},$$
$$-\frac{\partial i}{\partial x} = C\frac{\partial v}{\partial t} + Kv_{C_0}\frac{(\xi-1)^2}{\xi} + kv_{C_0}\frac{\partial}{\partial t}2(\xi-1-\log\xi),$$

where

$\xi = v/v_{C_0} (\geq 1),$

v_{C_0}: corona voltage,

$K = k(f+25) = \sigma_G\sqrt{r/2h}\times 10^{-11}[\mho/m],$ (6)

$k = \sigma_C\sqrt{r/2h}\times 10^{-11}[F/m],$

f : frequency $[s^{-1}]$,

r, h: conductor radius and height $[m]$,

$\sigma_G = \sigma_C(f+25),$

σ_C : corona loss constant.

If the two kinds of $\xi-\eta$ curves, which are given by relations $\eta=(\xi-1)^2/\xi$ and $\eta=2(\xi-1-\log\xi)$, are linealized piecewise by the two continued rectilinear segments respectively, the ν-th element of the approximate equivalent circuit of a single-conductor system with the corona loss elements becomes as illustrated in Fig. 3, where $\nu=1, 2, \cdots, n$,

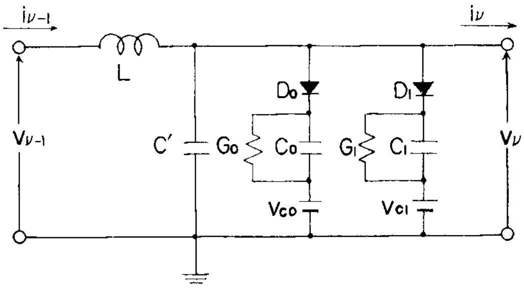

Fig. 3. The ν-th element of an approximate equivalent circuit of a single-conductor system with corona loss elements.

G_1, G_2: equivalent leakances[1],

C_0, C_1: equivalent capacitances[2],

v_{C_1}: voltage at intersection of picewise rectlinear characteristics.

But, if the value of the line voltage may transiently become both the positive and negative, though it is assumed to be always positive in our case, we must add the inverse-polarity and hysteresis elements to the corona loss ones, in Fig. 3.

Next respecting to the equivalent circuit element shown in Fig. 3, we conveniently define modes 0, 1 and 2 as follows:

$$\left.\begin{aligned} &\text{Circuit mode in } 0\leq v_\nu<v_{C_0} = \text{mode } 0,\\ &\text{Circuit mode in } v_{C_0}\leq v_\nu<v_{C_1} = \text{mode } 1,\\ &\text{Circuit mode in } v_{C_1}\leq v_\nu = \text{mode } 2, \end{aligned}\right\} \tag{7}$$

where it is, too, assumed that the value of the transient voltage is positive.

Now we can introduce the fundamental difference equations to connect the voltages and currents in the three modes 0, 1 and 2 of the ν-th element. Namely

(i) Mode 0:—

From Eq. (5), we have

$$\left.\begin{aligned} i_\nu &= a^0_{2\nu}v_\nu+b^0_{2\nu},\\ v_\nu &= a^0_{2\nu-1}i_{\nu-1}+b^0_{2\nu-1}, \end{aligned}\right\} \tag{8}$$

(ii) Mode 1:—

From Eqs. (6) and (7) and Fig. 3, we can derive the following equations:

$$\left.\begin{aligned} &L'\frac{di_{\nu-1}}{dt} = v_{\nu-1}-v_\nu\,, \\ &C'\frac{dv_\nu}{dt}+C_0\frac{d(v_\nu-v_{C_0})}{dt}+G_0(v_\nu-v_0) = i_{\nu-1}-i_\nu\,. \end{aligned}\right\} \tag{9}$$

By the same treatment as in the case of mode 0, we obtain

$$\left.\begin{aligned} i_\nu &= \frac{\Delta t}{L'+a^1_{2\nu+1}\Delta t}v_\nu+\frac{L'i^0_\nu-b^1_{2\nu+1}\Delta t}{L'+a^1_{2\nu+1}\Delta t} \\ &\quad(\equiv a^1_{2\nu}v_\nu+b^1_{2\nu})\,, \\ v_\nu &= \frac{\Delta t}{(C'+C_0)+(G_0+a^1_{2\nu})\Delta t}i_{\nu-1} \\ &\quad+\frac{(C'+C_0)v^0_\nu+(G_0v_{C_0}-b^1_{2\nu})\Delta t}{(C'+C_0)+(G^0+a^1_{2\nu})\Delta t} \\ &\quad(\equiv a^1_{2\nu-1}i_{\nu-1}+b^1_{2\nu-1})\,, \end{aligned}\right\} \tag{10}$$

(ii) Mode 2:—

By the same process as in the case of mode 1, we have

$$\left.\begin{aligned} i_\nu &= \frac{\Delta t}{L'+a^2_{2\nu+1}\Delta t}v_\nu+\frac{L'i^0_\nu-b^2_{2\nu+1}\Delta t}{L'+a^2_{2\nu+1}\Delta t} \\ &\quad(\equiv a^2_{2\nu}v_\nu+b^2_{2\nu})\,, \\ v_\nu &= \frac{\Delta t}{(C'+C_0+C_1)+(G_0+G_1+a^2_{2\nu})\Delta t}i_{\nu-1} \\ &\quad+\frac{(C'+C_0+C_1)v^0_\nu+(G_0v_{C_0}+G_1v_{C_1}-b^2_{2\nu})\Delta t}{(C'+C_0+C_1)+(G_0+G_1+a^2_{2\nu})\Delta t} \\ &\quad(\equiv a^2_{2\nu-1}i_{\nu-1}+b^2_{2\nu-1})\,. \end{aligned}\right\} \tag{11}$$

Substituting the numerical values of the line constants, terminal conditions etc. into Eqs. (8), (10) and (11) deduced as above, we can execute the numerical calculations with a digital computer. However, in process of digital computer calculations, the equivalent circuit elements may change from a mode to another, when the values of the element voltages increase or decrease. In the Appendix we shall illustrate the criteria of the mode transitions.

3. Numerical Analysis of Tower Voltage Rise due to Lightning Stroke on Overhead Ground Wire

In this chapter, we refer to the digital analysis of the transient voltages of the towers due to the lightning stroke on overhead ground wire, as one practical application of the previously described numerical computation. Now Fig. 4 illustrates a single-conductor system consisting of the single ground wire and the transmission towers to hold it, which the authors bring up as a subject to be analysed. Though in practice the transmission systems are the multi-conductor ones and the surges along the ground wire are necessarily influenced by the power lines, in this paper they neglect the induction effects owing to the lines and only consider the single-conductor system as shown in Fig. 4, in order to simplify the calculations.

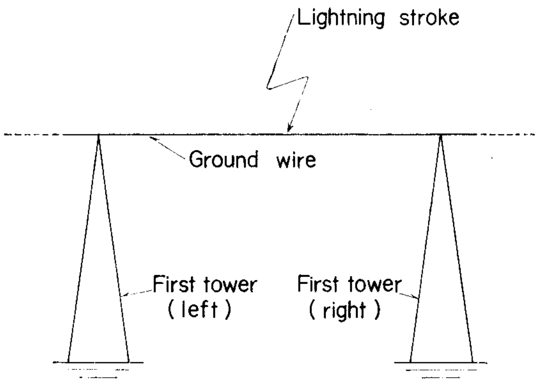

Fig. 4. Illustration of lightning stroke against overhead ground wire.

Next, by the aid of the equivalent circuit element given in Fig. 3 and the equivalent circuit[7] of the tower equipped with the counterpoise to reduce the earthing resistance, we can obtain the approximate equivalent circuit of the system in Fig. 4 as shown in Fig. 5, where

$\boxed{S_{10}}$, $\boxed{S_{20}}$: elements substituted $L'/2$ for L' in Fig. 3,

$\boxed{S_{1\nu}}$, $\boxed{S_{2\mu}}$: same elements as sketched in Fig. 3,

$\nu = 1, 2, \cdots, n, \quad \mu = 1, 2, \cdots, m-n,$

z : surge impedance of ground wire,

Z_0 : stroke channel impedance,

R_T : resistance to determine initial value of tower impedance,

L_T : equivalent tower inductance,

R_E : resistance to decide initial value of surge impedance of tower foot with counterpoise,

L_E : equivalent inductance of tower foot with counterpoise,

R_G : earthing resistance,

v_{1n}, i_{1n}, v_{1t}, i_{1t} $(=i_{1G})$ and others: voltages and currents as shown in the figure.

As seen in the figure, the corona loss on the ground wire further than the two first towers on the left and right sides of the stroke point, say the first towers, and the influences after the second tower are assumed to be neglected. Hence the ends of the ground wire on the both sides of the first towers may be grounded with the surge impedance z. As in the preceeding chapter we already discussed the numerical computation of the travelling waves on the single line radiating corona, in this chapter we shall develop a digital analysis of the performances of the voltages and currents at the transition points, namely the stroke point and the towers.

First let us refer to the lightning current I. This should be a forced current flowing down along the main stroke channel, whose value is I, by the definition. However upon the waves, which come into the stroke point along the ground wire after reflected at the towers, the channel operates as a conductor of the surge impedance Z_0, therefore the stroke current must not be thought to be supplied from a simple forced current source. Moreover the corona phenomena belong to a nonlinear matters and so reject the superposition theory, hence in a strict sense, we cannot separate the incident, refracted and reflected waves at the transition points. Accordingly it is perhaps impossible to analyse very exactly the effects of the stroke current in numerical calculation. So the authors, as one approach, assume the equivalent lightning voltage source of the magnitude V, which let flow the current of the sum I into the right and left parts of the ground wire from the stroke point. Due to this assumption the V becomes

(i) For mode 0:—

$$V = I(Z_0+z/2) = I_0(Z_0+\sqrt{L/C}/2). \tag{12$_0$}$$

(ii) For mode 1:—

$$V = I\{Z_0+\sqrt{L'/C'+C_0}/2\}. \tag{12$_1$}$$

(iii) For mode 2:—

$$V = I\{Z_0+\sqrt{L'/C'+C_0+C_1}/2\}, \tag{12$_2$}$$

where the equivalent leakances are neglected and only the equivalent capacitances are considered.

Using the V's given Eqs. $(12)_0 \sim (12)_2$, we can draw an equivalent circuit to express the relation between the V and the system, which is shown in Fig. 5. From the figure the relations between the V and the stroke point voltage v_0 are obtained as follows:

$$\left.\begin{aligned} v_0 &= V - Z_0 I, \\ I &= i_{10} + i_{20}. \end{aligned}\right\} \tag{13}$$

On the other hand, from Eqs. (8), (10) and (11) i_{10} and i_{20} are

$$\left.\begin{aligned} i_{10} &= a_{10}^s v_0 + b_{10}^s, \\ i_{20} &= a_{20}^s v_0 + b_{20}^s, \\ s &= 0, 1, 2. \end{aligned}\right\} \tag{14}$$

With Eqs. (13) and (14), we have

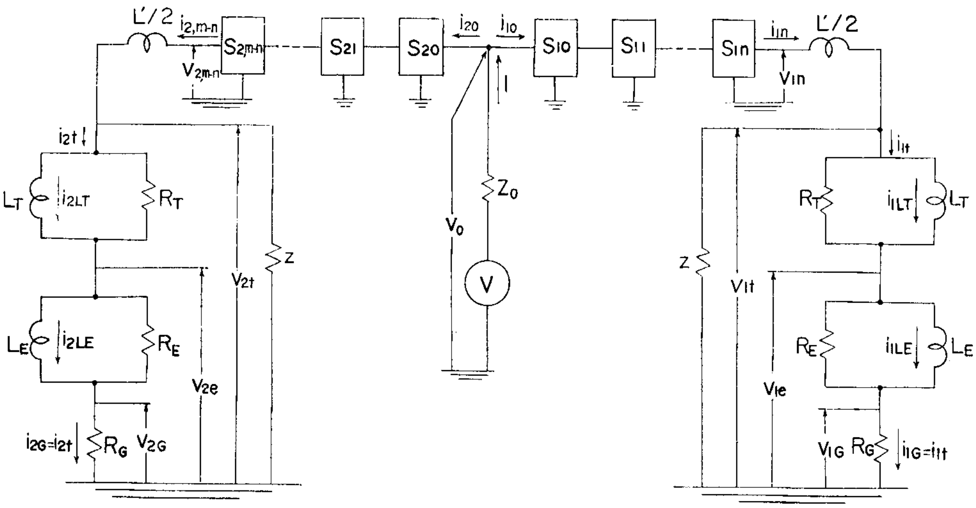

Fig. 5. An approximate equivalent circuit of the system shown in Fig. 4.

$$v_0 = \frac{V - Z_0(b_{10}^s + b_{20}^s)}{1 + Z_0(a_{10}^s + a_{20}^s)}. \tag{15}$$

Next, for instance, the relations between the voltages and currents at the right towers shown in Fig. 5, are given by the following difference equations.

$$\left.\begin{aligned} v_{1n} - v_{1t} &= L'(i_{1n} - i_{1n}^0)/2\Delta t, \\ i_{1n} - i_{1t} &= v_{1t}/z, \\ v_{1n} - v_{1e} &= R_T(i_{1t} - i_{1LT}) = L_T(i_{1LT} - i_{1LT}^0)/\Delta t, \\ v_{1e} - v_{1G} &= R_E(i_{1t} - i_{1LE}) = L_E(i_{1LE} - i_{1LE}^0)/\Delta t, \\ v_{1G} &= R_G i_{1G} = R_G i_{1t}, \\ i^0 &= i|_{t-\Delta t}, \ t - \Delta t \geq 0. \end{aligned}\right\} \tag{16}$$

Modifying these equations, finally we can reduce the following relations.

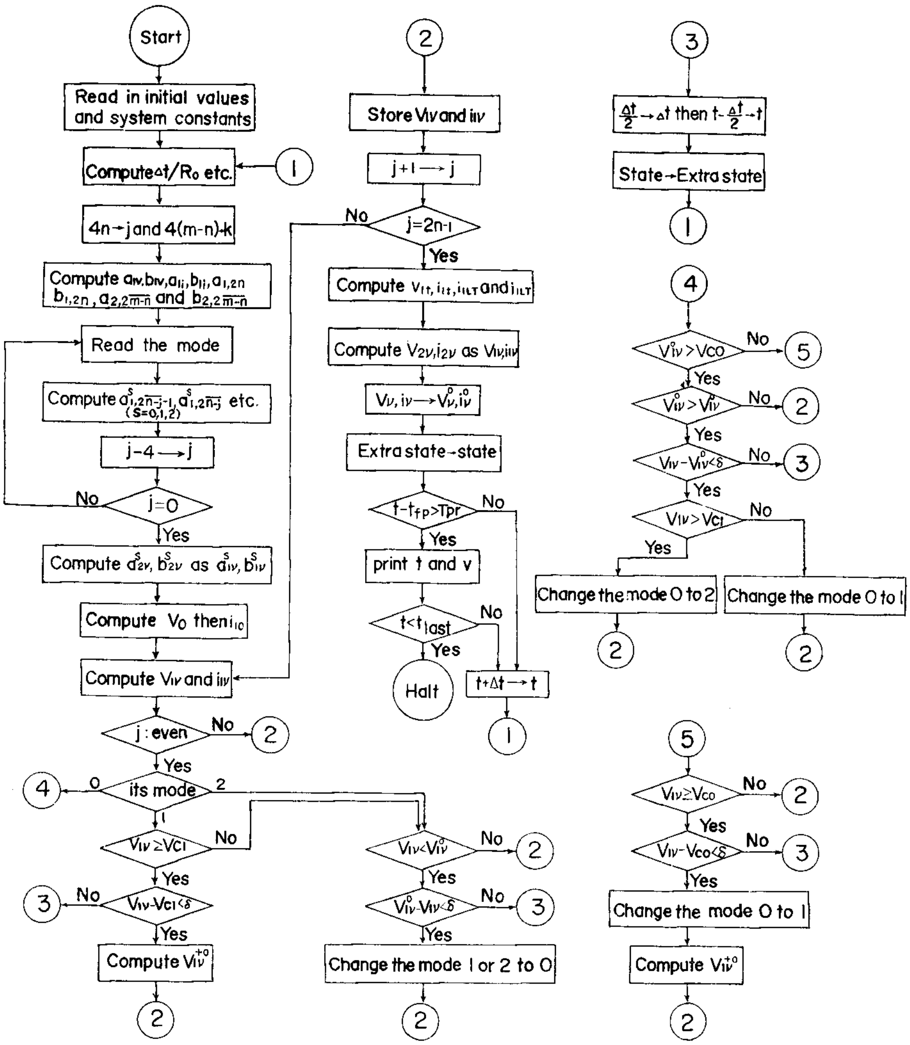

Fig. 6. Digital computer flow-chart.

$$
\left.\begin{aligned}
i_{1LT} &= \frac{R_T\Delta t}{R_T\Delta t+L_T}i_{1t}+\frac{L_T}{R_T\Delta t+L_T}i^0_{1LT}, \\
i_{1LE} &= \frac{R_E\Delta t}{R_E\Delta t+L_E}i_{1t}+\frac{L_E}{R_E\Delta t+L_E}i^0_{1LE}, \\
i_{1t} &= \frac{v_t}{Z_t}+\frac{1}{Z_t}(Z_Ti^0_{LT}+Z_Ei^0_{LE}) \\
&\quad (\equiv a_{1i}v_t+b_{1i}), \\
v_{1t} &= \frac{1}{a_{1i}+1/z}i_{1n}-\frac{b_{1i}}{a_{1i}+1/z} \\
&\quad (\equiv a_{1v}i_n+b_{1v}),
\end{aligned}\right\} \tag{17}
$$

$$i_{1n} = \frac{2\Delta t}{2a_{1v}\Delta t + L'}v_{1n} + \frac{L' i^0_{1n} - 2b_{1v}\Delta t}{2a_{1v}\Delta t + L'}$$

$$(\equiv a_{1,2n}v_{1n} + b_{1,2n}),$$

where

$$Z_t = Z_T + Z_E + R_G,$$
$$Z_T = R_T L_T/(R_T\Delta t + L_T),$$
$$Z_E = R_E L_E/(R_E\Delta t + L_T).$$

The same relations come into being about the left tower.

If the numerical values of the lightning currents, the channel impedance, the various constants respect to the wire and tower, and the other main quantities are given, the values of the transient voltages and currents on the ground wire and the first towers are able to be numerically calculated by using Eqs. (8), (10)~(15) and (17) obtained in the preceeding and present chapters. Lastly, a digital computer flow-chart are drawn in Fig. 6.

4. Numerical Examples

In this chapter the authors shall discuss some numeric examples of the tower voltage rise due to the lightning stroke on the ground wire as already shown in Fig. 4. Here they assume the numerical values of the system parameters as tabulated in Table 1, where the ones of σ_C and σ_G were inferred from the computation by their surge analyser[4] for the positive-porality surge with the wave form of $0\times 20\mu s$[4], and the other conditions are fairly reasonable with respect to the practical transmission systems[7].

The transient performance of the first tower voltage v_{1t} or v_{2t} after the instant, when the lightning strikes the ground wire at the midspan, is plotted in Fig. 7, where the full and dotted lines correspond to the cases considering and neglecting corona loss respectively, for the latter of which the numerical calculations are carried out by means of the conventional travelling wave theory. In this case, the first tower voltage v_{1t} or v_{2t} becomes, at first,

$$v_{1t},\ v_{2t} = \{0.75\varepsilon^{-0.347(t-0.5)} + 4.28\varepsilon^{-0.847(t-0.5)} + 4.90\varepsilon^{-7.75(t-0.5)}\}10^3 H(t-0.5)\quad [KV];\ t[\mu s]$$

From the figure it is seen that the surge crest is in fairly large rate damped due to corona loss, although it be considered that the third term in the right side of the above equation should be perhaps very rapidly dissipated by the ohmic losses of the ground wire and ground return, say skin effects. In the connection, the spike due to the third term should be, in fair rate, shaved[4] by reason of using the $L'-C'$ elements of a finite number as the original delay circuit, as if by the skin effects. But, the detail of these problems we wish to keep for the next opportunity.

Table 1. Numerical conditions assumed to analyse the circuit shown in Fig. 5.

Hight of ground wire : h	30 [m]
Radius of ground wire : r	1.2×10^{-3} [m]
Lumped distance : Δx	15 [m]
Surge impedance of return stroke channel : Z_0	400 [Ω]
Surge impedance of ground wire : z	553 [Ω]
Inductance of ground wire : L'	27.6 [μH/Δx]
Capacitance of ground wire : C'	90.5 [$\mu\mu$F/Δx]
Span length : S	400 [m]
Number of equivalent circuit elements : m	20
Corona loss constant about wave distotion : σ_C	40
Corona loss constant about wave attenuation : σ_G	4.5×10^6
Equivalent capactitance : C_0	24 [$\mu\mu$F/Δx]
〃 : C_1	48 [$\mu\mu$F/Δx]
Equivalent leakance : G_0	1/494 [m℧/Δx]
〃 : G_1	1/247 [m℧/Δx]
Corona voltage : v_0	140 [KV]
Intersection voltage : v_1	238 [KV]
Resistance to decide initial value of tower impedance : R_T	100 [Ω]
Equivalent tower inductance : L_T	10 [μH]
Resistance to decide initial value of tower-foot impedance with counterpoise : R_E	50 [Ω]
Equivalent inductance of tower-foot with counterpoise : L_E	50 [μH]
Earthing resistance : R_G	10 [Ω]
Lightning current : I	9.8(0×20μS) [KA]
Time duration : Δt	0.02 [μs]

Next Fig. 8 shows the maximum tower voltages $v'_{1t\ \max}$ s or $v'_{2t\ \max}$ s, when the lightnings strike the ground wire at distances of 30, 60, 90, 120, 150, 180, 210, 240 and 270 meters from the first tower respectively, and the time lags from the instant, when the first incident wave reaches the tower, to the appearance of the maximum voltages. As seen in Figs. 7 and 8, in any case the tower voltage arrives to the maximum before the instant, when it will be estimated that the wave reflected at the stroke point again comes back

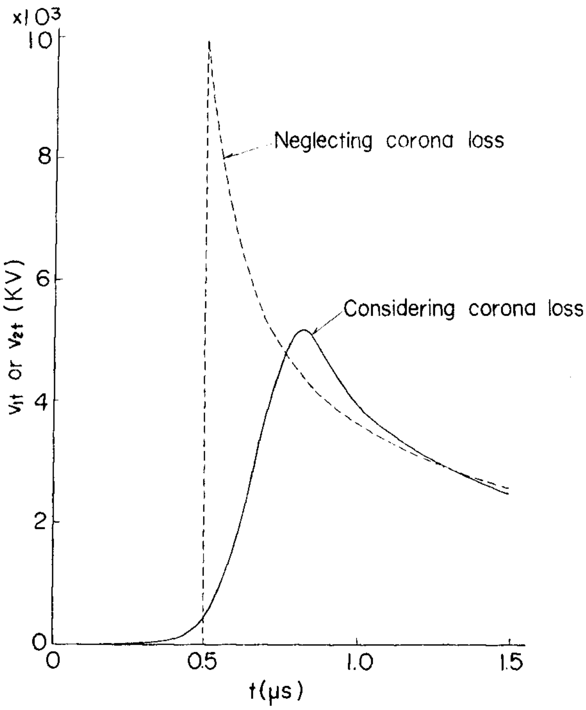

Fig. 7. Transient performance of v_{1t} or v_{2t}.

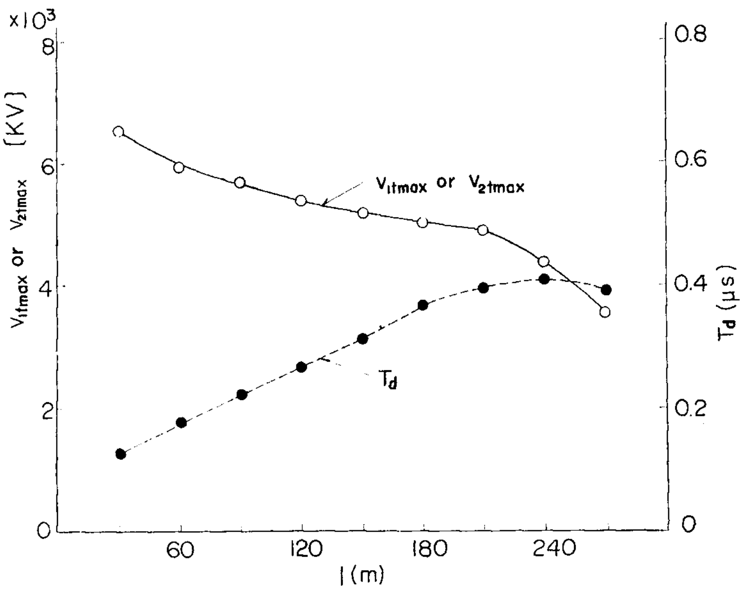

Fig. 8. $v_{1t\max}$ or $v_{2t\max}$ and T_d vs. l.

at the tower, and the more the stroke point nears to the tower, the larger the maximum voltage becomes.

5. Conclusion

In the preceding charpters have been illustrated a new numerical analysis of the attenuation and distortion of the surges due to corona discharges on a single-conductor system and one application of the theory to the matter of transient performances of the tower voltages caused by the lightning stroke on the overhead ground wire. In addition, though here we have treated only the single-conductor systems, in the future we intend to investigate the more practical transmission systems, say the multi-conductor ones.

References

1) S. Hayashi, J. Umoto, S. Machida: Convention records at the annual meeting of I. E. E. J., No. 565, May (1958).
2) S. Hayashi, J. Umoto: Convention records at the annual meeting in Kansai District of I. E. E. J., No. 98, Oct. (1958).
3) S. Hayashi, J. Umoto, E. Nakamura: Ibid, No. 9-9, Nov. (1964).
4) E. Nakamura: Master thesis, March (1965).
5) C. F. Wagner: T. A. I. E. E., **73**, 858 (1955).
6) K. Ishihara: Simposium records at the annual meeting in Kansai District of I. E. E. J., No. 7-3, Nov. (1965).
7) S. Hayashi, J. Umoto: J. I. E. E. J., **84**, 1114~1121 (1964).

Appendix Criteria of Mode Transitions

As described in Chapter 2, when the voltage v_ν ($\nu=1, 2, \cdots, n$) of the ν-th element of the equivalent circuit increases or decreases, it will often vary from a mode to another. Here we can think of the several reasonable criteria of the mode variations as follows:

(i) If $v_\nu \geq v_{C_0}$ in the preceding mode 0, the new mode should be 1,
(ii) If $v_\nu \geq v_{C_1}$ in the mode 1, the new mode 2,
(iii) If $v_\nu < v_\nu^0$ in the mode 1, the new mode 0,
(iv) If $v_\nu < v_\nu^0$ in the mode 2, the new mode 0,
(v) If $v_{C_0} < v_\nu^0 < v_\nu < v_{C_1}$ in the mode 0, the new mode 1,
(vi) If $v_{C_1} < v_{\nu 0}^0 < v_\nu$ in the mode 0, the new mode 2.

In this connection, if the difference of v_ν and v_ν^0 become larger than a small constant, the digital computer flow-chart is drawn up so that the smaller time difference Δt may be selected to decrease the former difference (see Fig. 6), and therefore it may be believed that the case of $v_\nu^0 < v_{C_0}$ and $v_\nu \geq v_{C_1}$ can't present itself.

Next, as the value of the equivalent capacitance of the equivalent circuit element changes before and after a mode transition, in order to carry out the calculation after the variation, we need to seek for the initial value v_v^{+0} of the second kind of the voltage v_v at the transition instant,. Accordingly let us search for v_v^{+0} in each transition hereafter.

(i) From mode 0 to 1:—

By the conservation law of electric charges, we have

$$C'v_v^{-0} = C'v_v^{+0} + C_0(v_v^{+0} - v_{C_0}).$$
$$\therefore \quad v_v^{+0} = \frac{C'}{C'+C_0} v_v^{-0} + \frac{C_0}{C'+C_0} v_{C_0}, \qquad \text{(App. 1)}$$

where

v_v^{-0}: initial voltage of the first kind.

(ii) From mode 1 to 2:—

By the same conservation low, we obtain

$$C'v_v^{-0} + C_0(v_v^{-0} - v_{C_0}) = C'v_v^{+0} + C_0(v_v^{+0} - v_{C_0}) + C_0(v_v^{+0} - v_{C_1}),$$
$$\therefore \quad v_v^{+0} = \frac{C'+C_0}{C'+C_0+C_1} v_v^{0} + \frac{C_1}{C'+C_0+C_1} v_{C_1}. \qquad \text{(App. 2)}$$

(iii) and (iv) From mode 1 or 2 to 0:—

As is well known, charge (q)-voltage (v) characteristic curve on a single conductor is roughly as shown in App. Fig. 1, where the upper line correspondes to the cases (iii) and (iv). However, in these cases, the relation $q = cv$ (c: conductor capacitance) doesn't come into being, and therefore the conservation law of charges can't be applied to the mode transitions. So in these cases, we determine to use the following relation

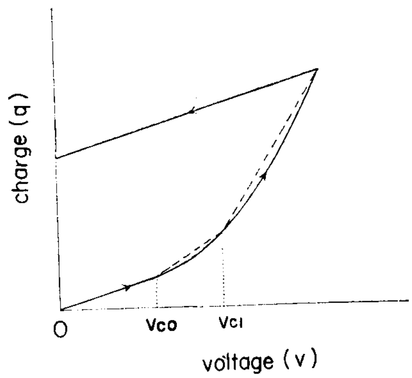

App. Fig. 1. $q-v$ curve of single conductor.

$$v_v^{+0} = v_v^{-0}. \qquad \text{(App. 3)}$$

(v) and (vi) From mode 0 or 1 to 2:—

These cases correspond to the ones, in which the voltage v begin to rise again after decreasing until a value. However the authors couldn't find the appropriate reports or new ideas for these cases. Also the conservation law of charges is not held, and therefore they again decided to make use of Eq. (App. 3).